SCIENCE CHINA
Earth Sciences

• RESEARCH PAPER •

June 2011 Vol.54 No.6: 924–935
doi: 10.1007/s11430-010-4109-6

Prediction of permafrost changes in Northeastern China under a changing climate

WEI Zhi[1,2,3], JIN HuiJun[1*], ZHANG JianMing[1†], YU ShaoPeng[1], HAN XuJun[4], JI YanJun[5], HE RuiXia[1] & CHANG XiaoLi[1]

[1]*State Key Laboratory of Frozen Soils Engineering, Cold and Arid Regions Environmental and Engineering Research Institute, Chinese Academy of Sciences, Lanzhou 730000, China;*
[2]*Northwest University for Nationalities, Lanzhou 730030, China;*
[3]*Baiyin Hydraulic Engineering Designing Institute, Baiyin 730900, China;*
[4]*Laboratory of Remote Sensing and Geospatial Science, Cold and Arid Regions Environmental and Engineering, Chinese Academy of Sciences, Lanzhou 730000, China;*
[5]*Gansu Electric Power Design Institute, Lanzhou 730050, China*

Received December 2, 2009; accepted May 4, 2010; publised online January 11, 2011

Northeastern China has the second largest expanse of permafrost in China, primarily known as Xing'an-Baikal permafrost. Located on the southeastern edges of the Eurasian cryolithozone, the permafrost is thermally unstable and ecologically sensitive to external changes. The combined impacts of climatic, environmental, and anthropogenic changes cause 3-dimensional degradation of the permafrost. To predict these changes on the southern limit and ground temperature of permafrost in Northeastern China, an equivalent latitude model (ELM) for the mean annual ground surface temperature (MAGSTs) was proposed, and further improved to take into account of the influences of vegetation and snow-cover based on observational data and using the SHAW model. Using the finite element method and assuming a climate warming rate of 0.048°C a^{-1}, the ELM was combined with the unsteady-state heat conduction model to simulate permafrost temperatures at present, and to predict those after 50 and 100 a. The results indicate that at present, sporadic permafrost occurs in the zones with MAGSTs of 1.5°C or colder, and there would still be a significant presence of permafrost in the zones with the present MAGSTs of 0.5°C or colder after 50 a, and in those of –0.5°C or colder after 100 a. Furthermore, the total areal extent of permafrost would decrease from 2.57×10^5 km^2 at present to 1.84×10^5 km^2 after 50 a and to 1.29×10^5 km^2 after 100 a, i.e., a reduction of 28.4% and 49.8% in the permafrost area, respectively. Also the permafrost would degrade more substantially in the east than in the west. Regional warming and thinning of permafrost would also occur. The area of stable permafrost (mean annual ground temperature, or MAGT⩽–1.0°C) would decrease from present 1.07×10^5 to 8.8×10^4 km^2 after 50 a, and further decrease to 5.6×10^4 km^2 after 100 a. As a result, the unstable permafrost and seasonally frozen ground would expand, and the southern limit of permafrost would shift significantly northwards. The changes in the permafrost environment may adversely affect on ecological environments and engineering infrastructures in cold regions. Avoidance of unnecessary anthropogenic changes in permafrost conditions is a practical approach to protect the permafrost environment.

permafrost, Northeastern China, climate change, equivalent latitude model (ELM), prediction

Citation: Wei Z, Jin H J, Zhang J M, et al. Prediction of permafrost changes in Northeastern China under a changing climate. Sci China Earth Sci, 2011, 54: 924–935, doi: 10.1007/s11430-010-4109-6

*Corresponding author (email: hjjin@lzb.ac.cn, jandb2009@live.cn)
†Equal contributor (email: zhangjm@lzb.ac.cn)

As a result of the energy exchange between the lithosphere and the atmosphere, permafrost is one of the most important components of the cryosphere. Permafrost can be a sensitive indicator of climatic and environmental changes, and these changes can be significantly amplified. Permafrost in the northern Da and Xiao Xing'anling (Hinggan) Mountains is mainly the result of latitudinal climate zonation, so-called the 'Xing'an-Baikal permafrost', where permafrost is better developed, i.e., colder and thicker at lower elevations in intermontane basins and lowlands, in contrast to elevational permafrost. It is susceptible to the impact of changes in climate and the external environment due to its location in the southeastern margin of the Eurasian cryolithozone. The main evidence of changes in permafrost incude the reduction in thickness, increasing ground temperatures, and the northward retreat of the southern limit of permafrost (SLP), which is the most obvious and direct indicator of a changing permafrost environment. Many studies have revealed multiple southward extensions and northward shrinkage of the SLP in Northeastern China since the Late Pleistocene. During the Last Glaciation Maximum (LGM, 32–16 ka BP), the SLP extended roughly along the 38°–40°N in the east to 37°–39°N in the west, and later it retreated northwards under a warming climate [1–5]. During the late 20th century, permafrost has retreated intensively and extensively, under the impacts of climate warming and human activities [6–12].

Research on permafrost in Northeastern China can be summarized into three main phases:

(1) In the late 1950s, permafrost research was initiated along with geological surveys, hydrogeological and engineering geological investigations, and many engineering explorations for civil design and construction [13, 14]. The SLP was preliminarily delineated. In the early 1970s, the 'Joint Taskforce for Studying Permafrost in the Da and Xiao Xing'anling Mountains' was organized by several institutions, and two field investigations were conducted. The SLP was redrawn, and the zonation of permafrost on the basis of areal continuity was proposed [15]. Significant progress was made on the understanding of the types and features of permafrost, resulting in a 'Map of Permafrost Distribution in Northeastern China' on a scale of 1:4000000. The zonation of permafrost largely reflects the effect of latitudinal climate zones and the influence of topography, vegetation, and soil water contents. In 1979 and 1980, specialists from similar institutions investigated permafrost twice in the northern Da Xing'anling Mountains. The position of SLP in Northeastern China was more refined. It followed approximately along the 0°C isotherm of mean annual air temperatures (MAATs), and zigzagged northwards and southwards between that of ±1.0°C [16, 17].

(2) In the early 1990s, geocryological studies were focused on those for the design and construction of civil infrastructures, and included mitigation and prevention of forest fires and frost hazards along highways, and for mining of placer gold [18, 19]. However, studies were very limited on assessment of the environmental impact and on the mitigative and adaptive measures for permafrost degradation or changes in cold environments.

(3) Since 2004, the 'CAS CAREERI 3rd term Innovation Program' was started, and the permafrost studies were undertaken, for the design and construction of the Russia-China Crude Oil Pipeline and the Mo'he Airport, the studies on permafrost and cold regions environments have been resumed and intensified. The scope and emphases underline the interactive and coupling processes among the engineering construction, permafrost environment, and climate change [20, 21].

The Northeastern China is one of the national key industrial, agricultural, and husbandry areas, and was or will be traversed by many completed and proposed projects in the important forested and pastoral areas in permafrost regions. Inevitably changes in the permafrost environment will inevitably have significant adverse impacts on to their safe operation [20, 22, 23]. Meanwhile, the Da and Xiao Xing'anling Mountains are areas with important forests, key wetlands, and crucial habitats. They have some of the most protected areas for many rare and endangered flora and fauna, which are very sensitive to the permafrost environmental changes [24–26]. The degradation of permafrost may profoundly affect the ecological environment in cold regions. Therefore, research on the permafrost environment in Northeastern China under a changing climate, especially those on the prediction of changes in the SLP, temperatures and thicknesses of permafrost, have important implications for the engineering infrastructures, environmental management and protection.

1 Study regions and methodology

1.1 Study region

Permafrost in Northeastern China is mainly latitudinal and concentratively found in the northern Da and Xiao Xing'anling Mountains north of 47°N, but elevational permafrost also occurs in the upper part and on the tops of mountain in the south, such as in the Changbai, Huanggangliang, and Arshan Mountains [6]. To fully understand the distribution and change of permafrost, the study region was selected to include the entire Northeastern China (Figure 1). Geomorphology is multifaceted in the study region with elevations ranging from about 100 to 2000 m. The region includes the northern Songnen Plain, the Da and Xiao Xing'anling Mountains, the Hulun Buir Sand Lands, and many large rivers such as the Heilong (Amur), Songhua, and Nen Rivers. The Da and Xiao Xing'anling Mountains cross the western and northeastern flanks in NE-SW and NW-SE directions, with the Nenjiang River Plain in between. In the southeast, the Changbai Mountain and others serve as the divide. The overall topography is higher in the

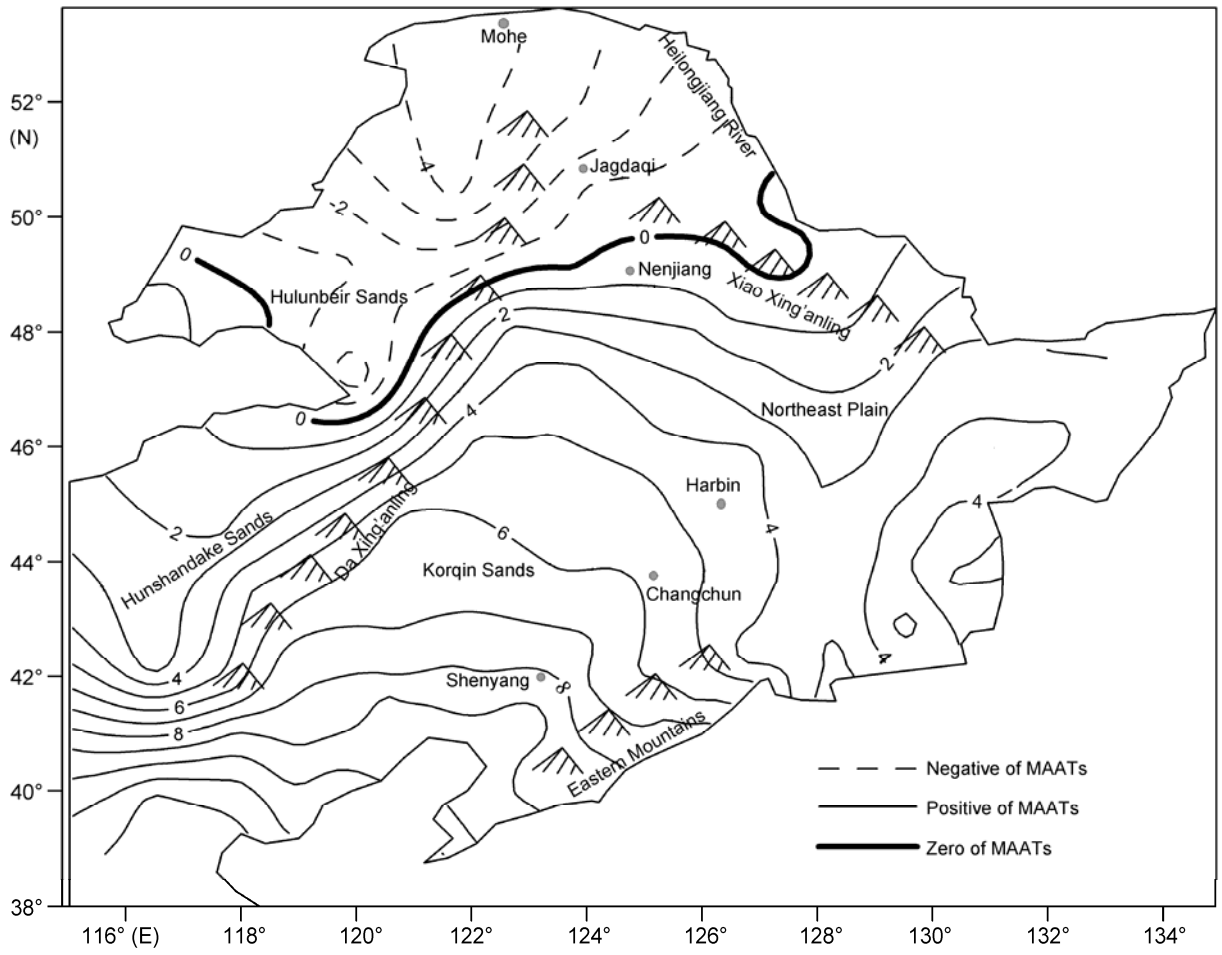

Figure 1 Topography and distribution of mean annual air temperatures in Northeastern China during 1975–2000.

east and west, and slightly lower in the central region.

The northern Da Xing'anling Mountains are 230 km long from southwest to northeast. They join the Xiao Xing'anling Mountains at the Yile'huli Mountains, which run in a west-east direction, and serve as a watershed divide between the Heilong and Nen Rivers. In the central section from Arshan to Yi'ershi and to the source of the Zhuo'er River, the mountain ranges have elevations between 1000 and 1400 m, which decrease northwards to 500–600 m in elevation in the region from Mangui to Gulian. In the south, the Da Xing'anling Mountains extend southwestwards into Hexigten Qi (Banner, or Prefecture) in the Inner Mongolia Autonomous Region, with its peak (2039 m) at the Mt. Huanggangliang. The mountain range is asymmetrical, with gentle western and steep eastern slopes. Large quantities of eroded debris from the steeper eastern slopes are carried to the Nen River Plain by deeply incised rivers. In contrast, the Xiao Xing'anling Mountains are gentle in topography, littered with meandering river courses at elevations of 500–600 m, and with a few peaks higher than 800 m.

The study region is characterized by a continental monsoonal climate in the cold- and northern cool-temperate climate zones. Due to the influence of alternating monsoons and ocean-inland high and low pressures, the climate is characterized by long, dry, and cold winters in comparison with short, moist, and hot summers; low MAATs, and large annual amplitudes in air temperatures. MAATs range northward from −1.0 to 1.0°C at the SLP (about 47°N) in the south, to −3.0 to −5.0°C in the north. The annual ranges of air temperature increase northwestwards from 40 to 50°C. The average annual precipitation decreases from 500–700 mm in the southeast to less than 200 mm in the northwest. The prevailing Siberian High Pressure in winter results in extensive and strong atmospheric temperature inversions, which weaken southwards [27]. In the Xing'anling Mountains, the inversion occurs at altitudes from 500 to 1000 m with a thermal gradient of about 10°C km^{-1} at Mohe, 8°C km^{-1} at Nenjiang, and 5°C km^{-1} at Hailar. The inversion greatly affects the development and distribution of the 'Xing' an-Baikal' permafrost. Wetlands, grasslands, forests, and permafrost inter-depend on and interact with each other, forming the northern forest-steppe landscapes.

1.2 Multi-model approach

At present, numerical models are generally adopted for predicting in the permafrost environment. These models are generally divided into three types. One is the analytical models of physical processes based on the theory of heat conduction. Because of its clearly defined physical significance, it has been extensively used in the studies on the interactions of permafrost and the engineering foundation [28, 29]. Another is the combination of analytical models and practical experience to establish semi-physical, semi-empirical models to predict permafrost changes. The third types are experimental analysis models based on field observation data to establish predictive statistical or empirical models [30]. With the rapid development and extensive applications of remote sensing (RS) techniques and geographic information systems (GIS) and other new technologies, permafrost prediction models have been increasingly coupled with the '3S' technologies.

In this paper, a GIS-supported equivalent-latitude model (ELM) for the mean annual ground surface temperatures (MAGSTs) in the study region was developed using meteorological data in Northeastern China to study the horizontal distributive features of permafrost and their changes. The boundary conditions for the model were jointly derived from the projected rates of climate warming from the prevailing general circulation models (GCMs) and long-term (50 a) trends of climate warming observed in meteorological stations. Then, using a finite element method, the unsteady-state heat conduction model was used to compute the changes in permafrost conditions at generalized 'points' under various boundary conditions. The ELM-predicted MAGSTs reflect the impact of global and local factors on ground surface temperatures, and the results from the unsteady-state heat conduction model reflects more the impact of geospatial features, such as soil types. More accurate geospatial predictions and the visualization of the predicted results for the purpose of mapping were realized by combining the statistical and physical models.

1.3 Equivalent latitude model (ELM) for MAGSTs

In contrast to those on the Qinghai-Tibet Plateau, the MAGSTs in Northeast China are affected not only by the solar radiation from its geographical location but also more by the thermal offsets induced by local factors, such as snow cover, vegetation, and moisture content of soils. Therefore, the ELM for the distribution of MAGSTs at 0 cm was established using the data from 47 meteorological stations in the study region and taking into account of the abovementioned major factors.

1.3.1 Effect of snow cover on MAGSTs

Northeastern China has large snowfalls with a significant presence and duration of snow cover. Therefore, the impact of snow cover on the surface and permafrost temperatures is pronounced and needs to be considered in modeling. Changes in ground surface temperatures can be greatly attenuated by snow cover, and the heat exchange is modulated between land surface and atmosphere through the insulation and change in surface albedo and turbulent fluxes in the snow layers. Relatively thick and stable snow cover can have a good insulation effect [31, 32], retarding the rapid and significant cooling in winter. However, the snow melting in early winter and late spring has a cooling effect due to the large amount of latent heat involved, retarding and dampening the changes in ground surface temperatures. The impact of snow on surface temperatures differs significantly with the thickness and duration of snow cover. Therefore, the weighted 'equivalent' processing method based on Anisimov & Nelson's concept of snow-water equivalent was employed in the evaluation of the thermal effect of snow cover (eq. (1)) [8]. It includes the combined impact of the snow depth, duration, intensity, and latitude on the snow melting.

$$Z_s = \sin^2 \varphi \left\{ \sum_{i=1}^{k} [(P_i / \rho_r)(k - i + 1)] / k \right\}, \quad (1)$$

where P_i stands for monthly snow depth (in cm) (i = 1, 2, …, k); ρ_r for relative snow density (assumed constant in this study); φ for north latitude (in (°)); and k for snow duration (in month).

For the snow depth, the Raster data set from 1978–2005 was used from the 'Environmental and Ecological Science Data Center for West China, National Natural Science Foundation of China' (http://westdc.westgis.ac.cn). It was inversed from the brightness temperature data of passive microwave remote sensing SMMR (1978–1987), and SSM/I (1987–2005), and consisted of 9930 ASCII code files with a ground surface resolution of 25 km. Each file represents a dataset for a daily snow depth in China. After the processing of these data files on snow depths, the data for the monthly average, monthly maximum, and annual maximum snow depths and annual duration of snow cover were obtained for the study area.

The results and analysis indicate that: 1) The first snow in Northeastern China usually appears in Ta'he north of Yilehuli Mountains in late October, and the last snow is in areas north of the 0°C MAATs isotherm (slightly north of 47°N) in the following April; 2) The maximum snow depth, with a mean annual maximum snow depth of 21–25 cm, appears in February, mainly in the latitudes of 49°–51°N, i.e., along the Yakeshi-Arshan in the west, and in the region south of Dayangshu, east of the Nuomin River, north of Bei'an and the Awang River in the east.

The files of monthly average snow depth were read with ArcGIS as separate layers for functional operation, and then the annual equivalent of snow depth is made available after calculation using eq. (1). The 'equivalent' maximum snow

depth is 45–50 cm with a distribution pattern similar to the multiyear average annual snow depth. Snow data were extracted from each meteorological station to conduct the statistical analysis.

1.3.2 Principal factors controlling or influencing the ground surface temperature

Although the MAATs and their annual ranges basically control the formation, evolution, and distribution of permafrost, these features are closely related to snow cover and precipitation/snowfall. These variables are not mutually independent; they are well correlated with latitudes, displaying regular features northwards or northwestwards [20]. Therefore, principal factor analysis was used in the model. The new factors are a linear combination of original input factors (Table 1). The first three main factors, contribute to 93.2% of total variance, i.e., their combination basically express the model. However, these three factors are difficult to be measured directly and efficiently. Therefore, latitude, longitude, and altitude were used to establish the statistical model for MAGSTs in Northeastern China because of their good correlations and their easy accessibility.

1.3.3 Model optimization

First of all, the effects of slope angle and aspect on the absorption of solar radiation and further on the permafrost temperature were assessed using the equivalent latitude model (ELM) (eq. (2)), in which these effects were transformed into the equivalent latitude on the basis of the actual latitude.

$$\varphi' = \sin^{-1}(\sin\theta\cos\kappa\cos\varphi + \cos\theta\sin\varphi), \tag{2}$$

where φ' stands for equivalent north latitude (°), θ for slope angle (°), κ for aspect (°), and φ for north latitude (°).

Larger errors of simulated values appear for the meteorological stations at higher elevations in comparison with those actually measured. The analysis shows that the deviations tend to gradually increase at stations higher than 250 m in elevation. In order to achieve a better simulation and to avoid model failure in the local grids with 0 or negative values in DEM, a segmented function was formulated to optimize the ELM (eq. (3)). Goodness of fit tests shows that after the optimization, the regression model achieved 96.5% of the total variance, which is higher than 91.2% for that of the unsegmented (Figure 2). Therefore, the optimized simulation reflects the actual MAGSTs better.

$$\begin{cases} T_s = 77.113 - 0.252\alpha - 0.843\beta - 0.002\gamma, & \text{elevation} \leqslant 250 \text{ m}, \\ T_s = 89.998 - 0.258\alpha - 1.093\beta - 0.006\gamma, & \text{elevation} > 250 \text{ m}, \end{cases} \tag{3}$$

where T_s stands for MAGSTs, α for east longitude (°), β for equivalent north latitude (°), and γ for elevation (m).

The DEM with a resolution of 1 km×1 km from the United States Geological Survey (http://www.usgs.gov) was used to form slope angle and aspect Raster files in ArcGIS

Table 1 Component matrix of principal (controlling and/or influencing) factors for MAGSTs

Impact factor		Longitude	Latitude	Elevation	Mean ann. air temp.	Ann. range (air temp.)	Weighted equivalent snow depth	Annual precipitation	Contribution to total var. (%)
Principal factor	1	0.488	0.955	0.174	0.910	0.928	0.743	0.545	52.4
	2	–0.357	0.108	0.911	0.047	0.056	0.088	0.402	29.1
	3	–0.743	0.129	0.142	0.401	0.301	0.131	0.251	11.7

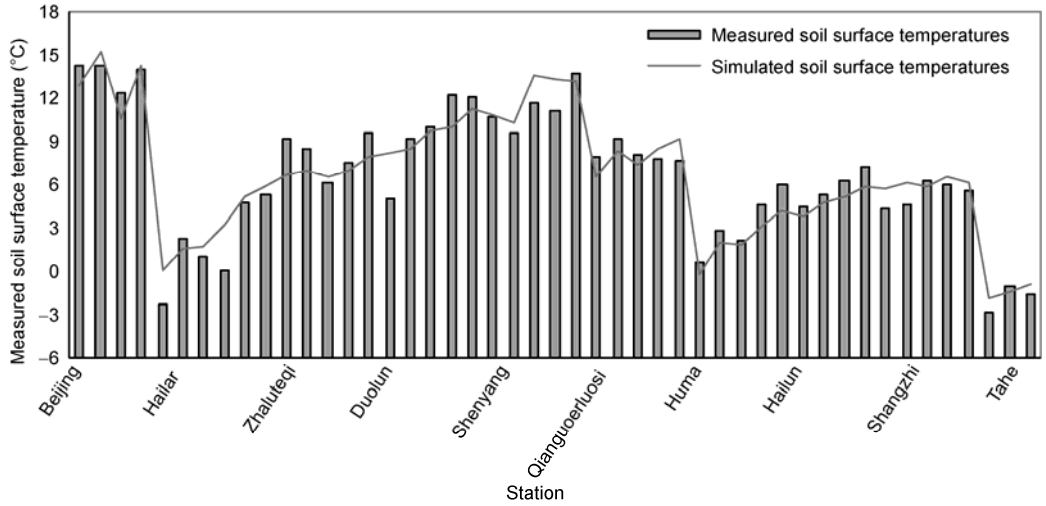

Figure 2 Comparison of the simulated and measured MAGSTs at the 47 meteorological stations in Northeastern China.

through the coordinate transformation. After extraction of slope angle and aspect data for meteorological stations, the ELM for MASGTs was built in GIS using C^{++} program.

1.3.4 Model adjustment for the influence of vegetation

Northeast China has the largest expanse of needle-leafed forests in China. The presence of vegetation, such as the coverage with the Xing'an larch (*Larix gmelinii*) and evergreen trees (mainly *Pinus sylvestris*), shrublands, meadows, turfed *Sphagmum* moss swamps, and feather (*Stipa*) grasslands, have a great influence on ground surface temperatures. Solar radiation is redistributed and transmitted between the soil, vegetation, and atmosphere, forming an integrated unity. Many land surface process models regard these three components as a whole to analyze moisture and heat exchanges among them, such as in the SPAC (Soil-Plant-Atmosphere Continuum) or SVAT (Soil-Vegetation-Atmosphere-Transfer) models. However, the impact of vegetation is a complex process as manifested in the effect of trees, shrubs, and litter on the radiation, wind speed, snow cover, and other factors. In July 2007, comparative measurements of shallow ground temperatures were made in a forest firebreak zone (i.e., a cutover land) and in the adjacent natural forest east of Beijicun (Arctic Village in China) in Mohe County, northern Heilongjiang Province. The results showed that the ground surface temperatures were about 3.5 to 6.2°C higher in the firebreak zone than in the natural forests [26].

Due to the complex impact of vegetation on heat transfer, the model simulation was applied to estimate the effects of vegetation on the ground surface temperature. In this study, the SHAW (Simultaneous Heat and Water, http://www.nwrc.ars.usda.gov/Models/SHAW.html) model was used, which was developed for simulating the ground freezing and thawing in a one-dimensional vertical profile from the plant crown canopy, snow, litter, and ground surface to a given depth of soil. The balance equations of energy and water fluxes at each layer can be written in implicit finite difference forms and can be simultaneously solved using the Newton-Raphson method.

After the model calibration for Tongyu Station for the period from the 181st to the 195th days in 2004, with the 2-h-interval data (http://www.eol.ucar.edu/projects/ceop/dm/), three representative sites, i.e., Tongyu, Sunwu and Tuli'he, at different latitudes and with varied vegetation types were selected for the modeling. Typical characteristics of the three stations are shown in Table 2. The three stations have the corresponding measurements in air and soil temperatures. In particular, Tongyu is a reference station for the International Energy and Hydrological Cycle Observing System Program (CEOP, Coordinated Enhanced Observing Period Data Management). The station has good observations of human activities, land-air exchange, terrestrial ecosystems, atmospheric compositions, and the boundary layer processes.

Simulation results show that in Northeastern China, effects of vegetation, especially trees and other tall vegetation, on ground surface temperatures differ in cold and warm seasons. The cooling effect dominates in the warm season, whereas the insulating effect is more evident in the cold season. The overall effect of vegetation on MAGSTs is a cooling of about 0.8–1.3°C. As a result, the annual thermal offset of vegetation for MAGSTs can be simplified as 1°C, the initial MAGSTs can be further adjusted, and the distribution of MAGSTs in Northeastern China can be revised accordingly (Figure 3).

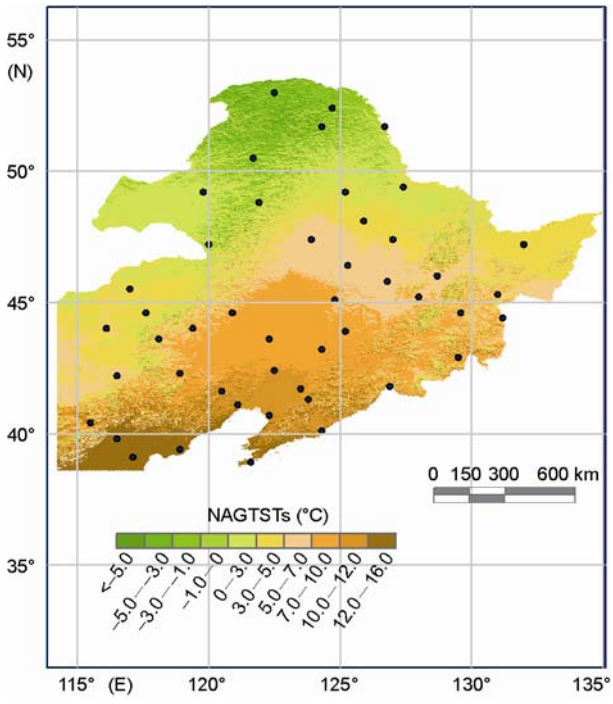

Figure 3 Distribution of the extrapolated MAGSTs in Northeastern China. Black dots are meteorological stations.

Table 2 Characteristics and results at the simulated sites

Station	Location	Vegetation type	MAATs (°C)	Frozen ground type	DMSM (°C) [a]
Tongyu	44.4°N, 122.9°E 184.0 m	Liao'he Plain with degraded grassland or croplands, grass statue at 5–10 cm	5.1	Seasonally frozen ground	–1.3
Sunwu	49.4°N, 127.4°E 235.1 m	Broad- and needle-leaved mixed forest in the northern Xiao Xing'anling Mts., mainly *Larix gmelinii* and white birch	–1.0	Island permafrost	–1.4
Tulihe	50.5°N, 121.7°E, 733.4 m	Needle-leaved forest of *Larix gmelinii* and *Pinus sylvestris* in the northern Da Xing'anling Mts., with shrubs and *Carex* in the underfloor	–4.0	Continuous permafrost	–0.8

a) The difference between the simulated and measured MAGSTs.

1.4 Unsteady-state heat conduction model

1.4.1 Regional climate change scenarios

The temperature distribution from the ELM for MAGSTs describes the initial upper boundary conditions of permafrost in Northeastern China. Its change is consistent with regional climate change with an offset of about 1.67°C at the land-air interface in the study region [11]. The regional climate change scenarios can be identified from the IPCC data center (http://www.mad.zmaw.de/IPCC_DDC) under three probable scenarios A2, A1B, and B1, in combination with the observed trend of climate warming (Table 3).

1.4.2 Unsteady-state heat conduction model

Assuming that there is only heat conduction and the ice-water phase change in the frozen soil; that heat convection and other processes are negligible [33]; and if the unfrozen water content is only a function of soil temperature, then the temperature of the permafrost can be described by a model of one-dimensional heat conduction with phase change (eqs. (4)–(6)).

$$\rho \cdot C \frac{\partial T}{\partial t} = \frac{\partial}{\partial x}\left(\lambda \frac{\partial T}{\partial x}\right) \tag{4}$$

and

$$C = \begin{cases} C_u, & T > T_p, \\ C_f + \dfrac{C_u - C_f}{T_p - T_b}(T - T_b) + \dfrac{L}{(1+W)}\dfrac{\partial W_i}{\partial T}, & T_b \leqslant T \leqslant T_p, \\ C_f, & T < T_b, \end{cases} \tag{5}$$

$$\lambda = \begin{cases} \lambda_u, & T > T_p, \\ \lambda_f + \dfrac{\lambda_u - \lambda_f}{T_p - T_b}(T - T_b), & T_b \leqslant T \leqslant T_p, \\ \lambda_f, & T < T_b, \end{cases} \tag{6}$$

where ρ stands for bulk density (kg m^{-3}) of soil; C for equivalent specific heat (J kg^{-1} K^{-1}) of frozen soils with phase change; C_u and C_f for the specific heat (J kg^{-1} K^{-1}) for unfrozen and frozen soils, respectively; λ for apparent conductivity (J m^{-1} h^{-1} °C^{-1}); λ_u and λ_f for thermal conductivity (J m^{-1} h^{-1} °C^{-1}) of unfrozen and frozen soils, respectively; L for latent heat (J kg^{-1}) of water; W and W_i for total moisture and ice contents (%), respectively; T_p and T_b for temperatures (°C) at the upper and lower boundaries with intense phase change, respectively; T for temperature variable (°C); t for time variable (h); and x for spatial variable (m) along the depth direction.

The geothermal gradient at the lower boundary in the permafrost is taken as 0.04°C m^{-1} [6, 34]. Measured permafrost temperatures indicate slight changes in the geothermal gradients at depths of 30–40 m in study region. Therefore, a depth domain of 60 m was taken in model calculation. The soils within the calculation depths were lithologically divided into three homogeneous and isotropic layers: 0–2.5 m, loamy sands; 2.5–10 m, silty clay; and 10–60 m, highly weathered granite. The physical and thermal parameters of the soils were obtained or assessed from permafrost surveys in Northeastern China, laboratory and on-site tests and tests on soil samples obtained from borings, hand-dug pits, and excavation sites during 2006–2009, and from the relevant literature and experience [35]. The upper boundary of ground surface temperature changes was given after climatic changes and seasonal variations in air temperatures (eq. (7)).

$$T = T_s + \alpha \cdot t + A\sin\left(\frac{2\pi \cdot t}{8760} + \frac{\pi}{2}\right), \tag{7}$$

where T_S stands for the MAGSTs (°C) at present; α for the linear change rate (°C a^{-1}) of the MAGSTs as a result of climate warming during the next 100 a (°C a^{-1}) and α = 0.048°C a^{-1}; t for the calculating time (h); A for physical amplitude of ground surface temperature from the measured data (half of what is measued), and A=18.5°C; and $\pi/2$ for the initial calculating phase (corresponding to the moment of highest surface temperature in a year).

2 Results and analysis

2.1 Results

To simplify the computation but still achieve sufficient accuracy, the interval of ground surface temperature calculated was set to 0.5°C. The steady state of the initial ground temperature field was obtained by ignoring the atmospheric warming, and taking a sinusoidal oscillation. The results calculated were shown in Table 4.

2.2 Changes in areal extent of permafrost

Under the projected climate change scenarios, permafrost as thick as 1.5 m may still exist under the conditions with pre-

Table 3 Projected and measured trends of climate changes for the study region

Scenario	A_2	A_1B	B_1	Measured	Chosen rate
Calculating mode	HADCM3	FGOALS-g1.0	CM1	1950–2000	
Linearly regressed warming rate in MAATs (°C a^{-1})	0.057	0.027	0.026	0.03–0.05	0.048

Table 4 Predicted changes in the permafrost environment under various MAGSTs[a)]

MAGSTs (°C)	At present	1.50	1.00	0.50	0.00	−0.50	−1.00	−1.50	−2.00
	50 a later	3.90	3.40	2.90	2.40	1.90	1.40	0.90	0.40
	100 a later	6.30	5.80	5.30	4.80	4.30	3.80	3.30	2.80
MAGT (°C)	At present	0.53	0.30	−0.06	−0.33	−0.58	−1.04	−1.45	−1.81
	50 a later	1.44	1.03	0.04	−0.30	−0.51	−0.80	−1.09	−1.39
	100 a later	3.26	2.79	2.15	1.16	−0.38	−0.58	−0.72	−0.90
Permafrost table (m)	At present	3.70	3.40	3.00	2.90	2.80	2.65	2.60	2.40
	50 a later	(3.20)	(3.30)	6.40	4.40	3.40	3.20	3.25	2.85
	100 a later	(2.30)	(2.30)	(2.75)	(2.70)	8.90	5.90	7.50	4.70
Permafrost depth (m)	At present	1.50	4.50	13.00	19.00	25.00	37.20	47.20	60.20
	50 a later	0.00	0.00	6.50	17.50	24.50	36.80	46.80	59.80
	100 a later	0.00	0.00	0.00	0.00	19.00	32.50	44.00	58.20

a) MAGT stands for mean annual ground temperature. The numbers in parentheses in the rows of the 'Permafrost table' are the maximum depths of seasonal frost penetration.

sent MAGSTs of 1.5°C. In areas with present MAGSTs of 0.5°C, permafrost as thick as 6.5 m may still remain after 50 a, and 100 a later, permafrost as thick as 19 m may still be there in the areas with MAGSTs colder than –0.5°C at present. Therefore, these three MAGSTs values were taken as the criteria for determining the occurrence of permafrost at present, and 50 and 100 a later. Contours of MAGSTs were obtained by data transformation of the model (Figure 4). Using the ArcGIS spatial computations, it is concluded that the total area of permafrost in Northeastern China will be reduced from the present 2.57×10^5 to 1.84×10^5 km^2 after 50 a (an areal reduction of 28.4% in comparison with present) and 1.29×10^5 km^2 after 100 a (a reduction of 49.8% in comparison with present). Moreover, the permafrost degradation displays a series of latitudinal successions and is more intense and rapid in the east.

The MAGSTs isotherm of 1.5°C coincides roughly with the present SLP. There is generally an 1.67°C difference between air and ground surface temperatures. Therefore, the local air temperature in the vicinity of the SLP should be around –0.17°C. This agrees well with findings that the SLP in Northeastern China fluctuates in the zone with MAATs of ±1.0°C and with an axis at about 0°C in the MAATs. This may, to a certain extent, confirm that the prediction is reasonably good. The predicted results could be further verified using the survey data along the Hei'he-Bei'an Highway in 2000. From Heihe (127.53°E, 50.22°N) to the Sunwu (127.50°E, 49.22°N) (K42–K190), there were 17 sections underlain by sporadic permafrost, where thick peat layer in the paludal meadows in the valleys and depressions serve as a buffer of permafrost to climate change. The permafrost temperature is about 0 to –0.1°C with thicknesses of 5 to 7 m [36].

2.3 Changes in permafrost temperatures

The temperature of permafrost, or MAGT, generally measured at a depth of 15 m, would increase generally, and the area of stable permafrost (MAGT≤–1.0°C) would decrease while that of unstable permafrost increases. The area of stable permafrost would decrease from the present 1.07×10^5 to 8.8×10^4 km^2 (a reduction of 17.8%) after 50 a, and further to 5.6×10^4 km^2 after 100 a (a reduction of 47.7%).

2.4 Changes in permafrost thickness

In general, permafrost, particularly very warm (MAGT ≥ –0.5°C) permafrost, would significantly decrease in thickness. The rate of decrease is greater than that of the deepening of the permafrost table due to additional lateral and upward degradation in warm permafrost [37].

The more intense and rapid degradation of permafrost degradation in the east may reflect the buffering effect of elevation, snow cover, and vegetation on the thermal stability of permafrost. Permafrost degradation would be less intense and slower in the middle Da Xing'anling Mountains with high elevations compared with that of the lower Xiao Xing'anling Mountains in the east although the precipitation is about the same.

3 Discussions

The boreal ecosystems in the Da and Xiao Xing'anling Mountains consist of forests, marshes, and grasslands, in which permafrost and the freeze-thaw processes play important roles in the heat, moisture, and nutrient cycles. The degradation of permafrost may cause destabilization, or even recession, of the boreal ecosystems that are interdependent on permafrost.

3.1 Resultant problems from permafrost degradation

3.1.1 Increase of greenhouse gas emissions

About 70% of total annual emissions of N_2O occur during

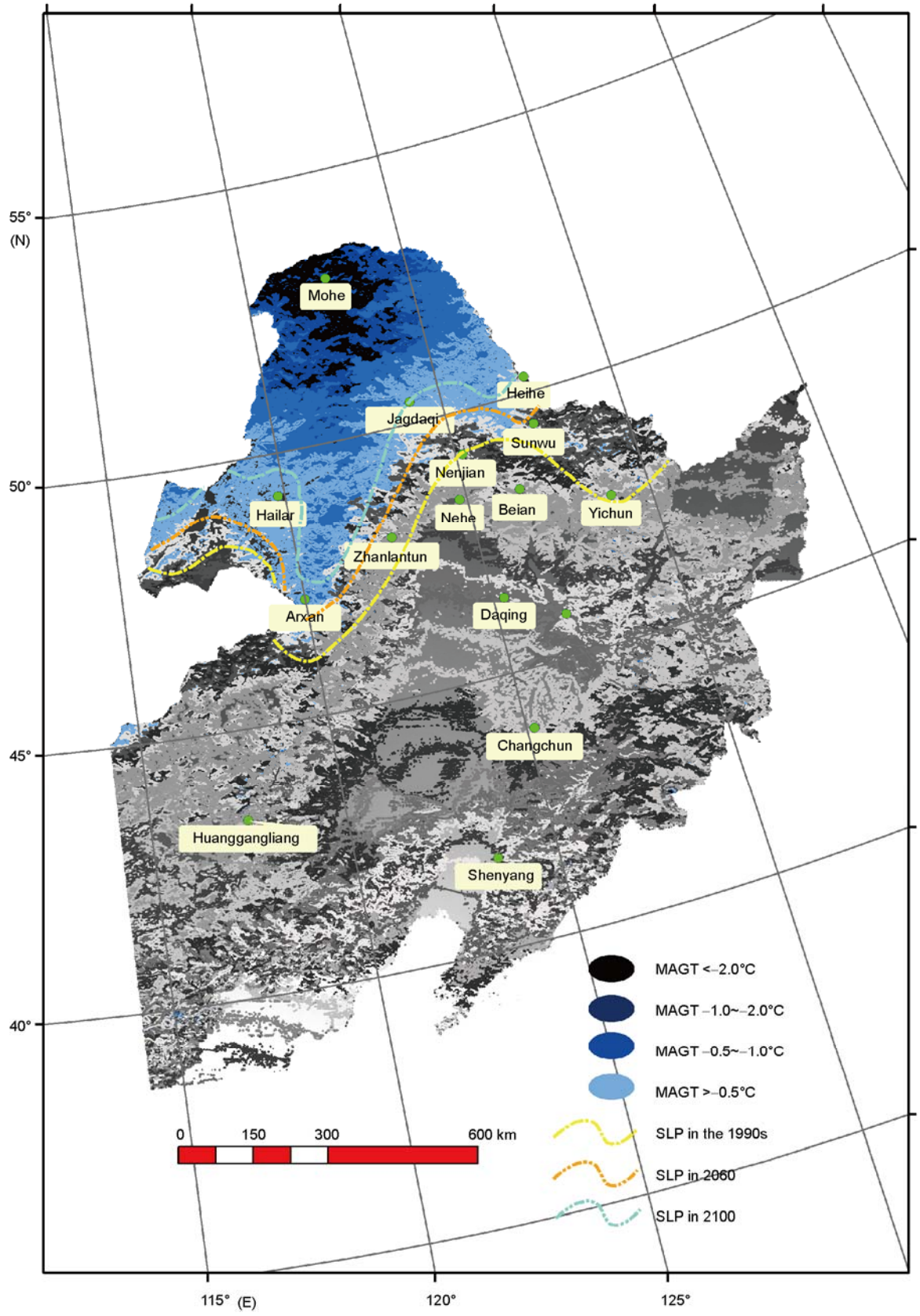

Figure 4 Predicted changes of the southern limit of permafrost and MAGTs in Northeastern China (Lambert projection) using the ELM for MAGSTs.

the thawing process of soils [38]. In the freezing process, a large amount of N_2O and CH_4 was sequestered beneath the top frozen layer [39]. The enriched layers gradually migrate downwards as the freezing fringe deepens, and the maximum concentrations at depths under the frozen layer gradually increase. In the thawing season, due to the lower organic contents in substrates, maximum concentrations of N_2O and CH_4 remain stable. When the frozen layer thaws completely, these gases move upwards and are released. As a result, the emissions of greenhouse gases peak, and the concentrations of N_2O and CH_4 under the permafrost decline sharply. Therefore, the thawing of frozen layer in Northeastern China may lead to concentrated release of the long-trapped N_2O and CH_4, positively feeding back to climate change.

3.1.2 Shrinkage of the wetland ecosystems

China's natural wetlands provide 54.9% of ecosystem services [40]. Northeastern China is one of the major areas (17.5%) for wetland resources in the nation, which are dominated by freshwater marshes and shallow lakes. The Da and Xiao Xing'anling Mountains region is one of the main wetlands areas in Northeastern China, where wetlands account for 95.5% and 92.7% of the forested area, respectively [41, 42]. Wetlands are developed mainly in valleys, gentle slopes, and lowlands near the water divides.

Due to the symbiosis of permafrost and wetlands [43], the degradation of permafrost would inevitably lead to the destabilization, or even shrinkage and drainage, of wetlands. In fact, the recession of wetlands has been taking place along with the degradation of permafrost [10, 25, 41]. Natural wetlands in Northeastern China had declined extensively during the periods from 1976 to 1986 and from 2000 to 2005 [44]. Field investigations in 2007 revealed that many wetlands near the SLP had been turned into farmlands; the original coniferous forests dominated by the cool-moist environment had been converted into an overlapping ecotone of agricultural and husbandry zones. For example, in the northernmost Beijicun (Arctic Village), Mohe County (MAATs at −5.0°C), wetlands around the meteorological station were cultivated as croplands, which accelerated soil erosion, leading to a continued, even sharply accelerated loss of soil nutrients [45, 46].

Precipitation in Northeastern China decreases northwards and northwestwards. It becomes less than 500 mm north of the central Da Xing'anling, and is further reduced to about 400 mm on the Hulun Buir Steppe in the northwest. The degradation of wetland ecosystems has caused the increasingly frequent droughts, land desertification, and dust storms, indicating that the cold regions' ecological environments in Northeastern China have changed.

3.1.3 Degradation of forest ecosystems

The lower or southern limit of mountain permafrost in Northeastern China is slightly lower or more southern than the timberline, with an elevational difference of 200–900 m. When permafrost degrades, the timberline of forests dominated by *Larix gmelinii*, *Pinus sylvestris,* and other species in the Da Xing'anling Mountains would retreat upwards or northwards. Bright coniferous forests would change gradually to mixed broad-leafed and coniferous forests [47]. For example, in Dayangshu Town, coniferous forests have been transformed to secondary forests consisting of dwarfed poplar and birch, probably as a result of the gradual disappearance of island permafrost since the 1960s. The succession of the dominant species has changed leaf-area index, resulting subsequently in a stronger heating of ground surfaces and leading to changes in soil moisture contents and temperatures.

3.1.4 Thaw slumps, thermokarsts, solifluctions, and other periglacial geohazards

Permafrost is significantly weakened upon warming and thawing, forming taliks and seasonally frozen ground, inducing pavement breakups, slope failure, and landslides due to thaw slumps and solifluctions. The occurrence of thermokarst lakes and drunken forests may increase in flatter areas. Moreover, because of the lost vegetative protection for the permafrost layer, seasonal thaw depth will further increase, and the degradation of permafrost can be accelerated.

3.1.5 Damages to the engineered infrastructures

Many infrastructures have been built on permafrost in northern Northeastern China. The shear strength and compressive modulus decreased sharply when permafrost thaws [48], leading to differential thaw settlement of foundation soils and consequently causing additional stress in the structures. These may pose threats to the safe operation of cold regions infrastructures.

3.2 Effects of other factors on the 'Xing'anBaikal permafrost'

In the Outer Baikalia in Eastern Siberia, the Far East and the Outer Xing'anling (Stanovoy) Mountains in Russia, and the Da and Xiao Xing'anling Mountains in China, an atmospheric temperature inversion occurs over wide areas in winter, affecting regions over thousands of kilometers, and is influential in the formation and maintenance of the 'Xing'an-Baikal permafrost' [1, 6, 25]. Due to climate warming and possible monsoon expansion, the Mongolia-Siberia High Pressure may have weakened, thus affecting the atmospheric temperature inversion. This may contribute significantly to the degradation of the 'Xing'an-Baikal permafrost'. However, due to the lack of data and research, it is too early to draw any reasonable conclusions on this issue.

4 Conclusions

During the next 100 a, permafrost degradation would occur

in Northeastern China due to warming climate. The more detailed manifestations would include the following:

The SLP would retreat northwards, and the permafrost area would shrink accordingly from present 2.57×10^5 to 1.84×10^5 km^2 after 50 a, i.e., an areal reduction of 28.4%, and 1.29×10^5 km^2 after l00 a (49.8% reduction in comparison with present areal extent of permafrost).

The MAGTs would increase, and the area of stable (MAGTs<–1°C) permafrost would be substantially reduced while areas of unstable permafrost and seasonal frozen ground would increase. The area of stable permafrost would decrease from the present value of 1.07×10^5 to 8.8×10^4 km^2 (17.8% reduction) after 50 a, and further to 5.6×10^4 km^2 (47.7%) after 100 a.

Overall, the thickness of permafrost would be on a decline, and the 3-dimensional (downward, upward, and lateral) degradation of very warm (MAGT≥–0.5°C) permafrost would become more evident. The thickness of the colder permafrost would decrease to a lesser extent, and it would be mainly caused by changes in the permafrost table, i.e., the downward degradation of permafrost.

The degradation of permafrost in Northeastern China may lead to adverse changes in the ecological environment, such as reduction of wetlands, further expansion of land desertification in the steppe zone (such as the Hulun Beir Prairie), and the succession of coniferous forests to the mixed broad-leafed and coniferous forests. It also may induce changes in local- and micro-climate and hydrologic and hydrogeologic environments through the complex interactions between the frozen ground, ecosystems, water, and atmosphere. Furthermore, it may substantially change the mechanical properties of frozen ground, impacting on the safety and long-term stability of the infrastructure.

The degrading of permafrost due to human interventions in cold region environments, such as anthropogenic alterations of surface canopies and drainage conditions, should be avoided or minimized if possible. In the vicinity of the SLP, permafrost is very sensitive to climate and environmental changes. Monitoring permafrost and cold region environments should be implemented and/or improved, in order to better assess these changes, to provide a timely warning in order to adapt and mitigate the adverse impacts of permafrost degradation, and manage and protect the cold regions environment in a sustainable way.

The authors are grateful to Ms. Lü Lanzhi of State Key Laboratory of Frozen Soils Engineering for her great support in climatic data analysis. Two reviewers provided constructive comments and insightful remarks, which have benefitted the authors in revising the paper. Senior Geotechnical Engineer Geoffrey Gay (retired) of University of Stuttgart, Germany generously edited the manuscript. Their generous assistance is thus acknowledged. This research was supported by National Natural Science Foundation of China (Grant Nos. 40821001 and 40701013), Chinese Academy of Sciences (CAS) Knowledge Innovative Program (Grant No. KZCX2-YW-311) and CAS 'One Hundred Talented People' Program.

1 Jin H J, Yu S P, Lü L Z, et al. Degradation of permafrost in the Da and Xiao Hinggan Mountains, Northeast China, and preliminary assessment of its trend (in Chinese). J Glaciol Geocryol, 2006, 28: 467–476
2 Cui Z J, Yang J Q, Zhang W, et al. Discovery of a large area of ice-wedge networks in Ordos: Implications for the southern boundary of permafrost in the north of China as well as for the environment in the latest 20 ka BP. Chin Sci Bull, 2004, 49: 1177–1184
3 Cui Z J, Xie Y Y. On the southern boundary of permafrost and periglacial environment during the late period of Late Pleistocene in north and northeast China (in Chinese). Act Geol Sin, 1984, 2: 165–176
4 Guo D X, Li Z F. Preliminary approach to the history and age of permafrost in northeast China (in Chinese). J Glaciol Geocryol, 1981, 3: 1–16
5 Dong G R, Gao S Y, Li B S, et al. The palaeo-periglacial phenomena and their signification in climate stratigraphy in Ordos Plateau from Late Pleistocene (in Chinese). Geogr Res, 1985, 4: 1–11
6 Zhou Y W, Guo D X, Qiu G Q, et al. Geocryology in China (in Chinese). Beijing: Science Press, 2000. 170–194
7 Jones P D, Wigley T M, Wright P B. Global temperature variations between 1861 and 1984. Nature, 1986, 322: 430–434
8 Anisimov O A, Nelson F E. Permafrost distribution in the Northern Hemisphere under scenarios of climatic change. Glob Planet Chan, 1996, 14: 59–72
9 Jin H J, Li S X, Wang S L, et al. Impacts of climatic change on permafrost and cold regions environments in China (in Chinese). Acta Geogr Sin, 2000, 55: 161–173
10 Jin H J, Yu Q H, Lü L Z, et al. Degradation of permafrost in the Xing'anling Mountains, Northeastern China. Permafrost Periglac Process, 2007, 18: 245–258
11 Wei Z, Jin H J, Zhang J M, et al. Modeling forecasting on permafrost changes in Northeastern China. In: Proceeding of 9th Int Conf on Permafrost, Fairbanks, Alaska, USA, 29 June to 3 July 2008. Fairbanks, Alaska, USA: University of Alaska Fairbanks, 2008. 1939–1944
12 Ding Y J. Recent degradation of permafrost in China and the response to climatic warming. In: Proceedings of 7th Int Conf on Permafrost, Yellowknife, NWT, Canada, 23–36 June 1998. University of Laval, 1998. 225–230
13 Ren Q J. Some new data about permafrost in Northeastern China (in Chinese). Hydro Eng Geol, 1957, (5): 10–14
14 Xin K D, Ren Q J. Permafrost distribution in northeastern China (in Chinese). Geol Knowledge, 1956, (10): 2–3
15 Guo D X, Wang S L, Lu G W, et al. Division of permafrost regions in the Da and Xiao Xing'anling Mountains of Northeastern China (in Chinese). J Glaciol Geocryol, 1981, 3: 1–9
16 The Study Committee of Permafrost in the Northeast China. Distributive characteristics of permafrost in Northeast China. In: Proceedings of 2nd Chinese Conf on Geocryol (in Chinese). Lanzhou: Gansu People's Press, 1983. 36–42
17 Lu G W, Wen B L, Guo D X. Geographical southern limit of permafrost in Northeastern China (in Chinese). J Glaciol Geocryol, 1993, 15: 214–218
18 Zhang B L, Wang C H, Cong C C. Preliminary study on renewable mechanism of placer gold in permafrost area in the northeastern Da and Xiao Xing'anling Mountains. In: Proceedings of 5th Chin Conf on Glaciol Geocryol (Vol 2) (in Chinese). Beijing: Science Press, 1996. 243–246
19 Zhao K Y, Zhang W F, Zhou Y W, et al. Impact of forest fire on environment in the Da Xing'anling Mountains and its mitigation (in Chinese). Beijing: Science Press, 1994. 1–150
20 Wei Z. Forecast on the changes of permafrost in Northeastern China and of the permafrost conditions for engineering geology along Mo'he-Daqing Crude Oil Pipeline route (in Chinese). Doctoral Dissertation. Lanzhou: Cold and Arid Regions Environmental and Engineering Research Institute, Chinese Academy of Sciences, 2008. 30–32
21 Wang T, Wang N L, Li S X, et al. Map of Glaciers, Frozen Ground and Deserts in China (1:4000000). Beijing: SinoMaps Press, 2005

22 Cheng G D. Influences of local factors on permafrost occurrence and their implications for Qinghai-Xizang Railway design. Sci China Ser D-Earth Sci, 2004, 47: 704–709
23 Wang G X, Yao J Z, Guo Z G, et al. Changes in permafrost ecosystem under the influences of human engineering activities and its enlightenment to railway construction. Chin Sci Bull, 2004, 49: 1741–1750
24 Brown R G E, Péwé T L. Distribution of permafrost in north America and its relationship to the environment: A review, 1963–1973. In: Permafrost: The North Amer Contrib to the 2nd Int Conf. Washington DC: Nat Acad Sci, 1973. 71–100
25 He R X, Jin H J, Lü L Z, et al. Recent changes of permafrost and cold regions environment in the northern Northeastern China (in Chinese). J Glaciol Geocryol, 2009, 31: 525–531
26 Chang X L, Jin H J, He R X, et al. Advances in permafrost and cold regions environments studies in the Da Xing'anling (Da Hinggan) Mountains, Northeastern China (in Chinese). J Glaciol Geocryol, 2008, 30: 176–181
27 Nekrasov I A, Klimovskii I V. Permafrost along the Baikal-Amur Main (Railway). Yakutsk: Science Press (Siberia Branch), 1978
28 Keller F. Automated mapping of mountain permafrost using the program PERMAKART within the geographic information system ARC/INFO. Permafrost Periglac Process, 1992, 3: 139–142
29 Li X, Cheng G D, Wu Q B, et al. Modeling Chinese cryospheric change by using GIS technology. Cold Reg Sci Technol, 2003, 36: 1–9
30 Li X, Cheng G D. A GIS-aided response model of high-altitude permafrost to global change. Sci China Ser-D Earth Sci, 1999, 42: 72–79
31 Zhang T, Osterkamp T E, Stamnes K. Effects of climate on the active layer and permafrost on the north slope of Alaska, U.S.A. Permafrost Periglac Process, 1997, 8: 45–67
32 Dai J B, Li A Y. Influence of snow cover to the ground temperature in the permafrost region in the northern part of the Great Xin'an Mountain (in Chinese). J Glaciol Geocryol, 1981, 3: 10–18
33 Esch D C. Thermal Analysis, Construction, and Monitoring Methods for Frozen Ground. Virginia: American Society of Civil Engineering, 2004. 239–254
34 Li Y W, Tong C J, Zhang L H. Computation of the permafrost thickness in Yituli'he observations field. In: Proceedings of 5th Chinese Conference on Glaciology and Geocryology (Vol. 2), 1996, August 18–22 (in Chinese). Lanzhou: Gansu Culture Press. 1143–1148
35 Xu X Z, Wang J C, Zhang L X. Physics of Frozen Soils (in Chinese). Beijing: Science Press, 2001. 151–155
36 Zhang Y, Wu Q B, Liu J P. Distribution characteristics of the permafrost in the section from Hei'he to Bei'an in the Xiao Hinggan Mountains (in Chinese). J Glaciol Geocryol, 2001, 23: 312–317
37 Jin H J, Zhao L, Wang S L, et al. Thermal regimes and degradation modes of permafrost along the Qinghai-Tibet Highway. Sci China-Ser D-Earth Sci, 2006, 49: 1170–1183
38 Rover M, Heinemeyer O, Kaiser E A. Microbial induced nitrous oxide emissions from an arable soil during winter. Soil Biol Biochem, 1998, 30: 1859–1865
39 Yu J B, Liu J S, Sun Z G, et al. Fluxes and controlling factors of N_2O and CH_4 emissions from freshwater marshes in Northeast China. Sci China-Earth Sci, 2010, 53: 700–709
40 An S Q, Li H B, Guan B H, et al. China's natural wetlands: Past problems, current status, and future challenges. Ambio, 2007, 36: 335–342
41 Wang Q B, Du M G. Current situation and prospect of wetland restoration in Northeast China. Forest Prospect Design, 2006, 140: 25–27
42 Li W H, Zhou X F, Liu X T. Strategic study on the protection of forests and wetlands and forestry development strategies in Northeastern China (Forestry Part). In: Shen G F, Shi Y L, eds. Study on Several Strategic Problems about Allocation of Water and Soil Resources, Ecology, Environmental Protection and the Sustainable Development in the Northeastern China (in Chinese). Beijing: Science Press, 2007. 1–418
43 Sun G Y. Discussion on the symbiotic mechanisms of swamp with permafrost—Taking Da and Xiao Hinggan Mountains as examples. J Glaciol Geocryol, 2000, 22: 309–316
44 Zhang S Q, Na X D, Kong B, et al. Identifying wetland change in China's Sanjiang Plain using remote sensing. Wetlands, 2009, 29: 302–313
45 Wang Z Q, Liu B Y, Wang X Y, et al. Erosion effect on the productivity of black soil in Northeast China. Sci China Ser D-Earth Sci, 2009, 52: 1005–1021
46 Liang A Z, Zhang X P, Yang X M, et al. Estimation of total erosion in cultivated Black soils in Northeast China from vertical profiles of soil organic carbon. Eur J Soil Sci, 2009, 60: 223–229
47 Xu W D. Preliminary study of correlations between distribution of main forest trees and thermal climate in northeast China (in Chinese). J Northeast Forest Inst, 1982, (4): 1–10
48 Liang B, Zhang G S, Liu D R. Experimental study on thawing subsidence characters of permafrost under frost heaving and thawing circulation (in Chinese). Chin J Geot Eng, 2006, 28: 1213–1217